Research in Pharmaceutical Sciences, December 2025; 20(6): 824-835
Received: 04-12-2024
Peer Reviewed: 19-01-2025
Revised: 08-04-2025
Accepted: 14-04-2025
Published: 15-11-2025

School of Pharmacy & Pharmaceutical Sciences
Isfahan University of Medical Sciences

Original Article

Prediction of new C-terminal Hsp90 inhibitors based on deguelin scaffold: homology modeling, virtual screening, QM/MM docking, MM/GBSA, and molecular dynamics simulations

Maryam Abbasi[1,2,*], Setareh Talaei[3], and Gholamreza Farshidfar[4]

[1]*Endocrinology and Metabolism Research Center, Hormozgan University of Medical Sciences, Bandar Abbas, I.R. Iran.*
[2]*Department of Pharmaceutical Chemistry, Faculty of Pharmacy, Hormozgan University of Medical Sciences, Bandar Abbas, I.R. Iran.*
[3]*Student Research Committee, Faculty of Pharmacy, Hormozgan University of Medical Sciences, Bandar Abbas, I.R. Iran.*
[4]*Department of Clinical Biochemistry, Faculty of Medicine, Hormozgan University of Medical Sciences, Bandar Abbas, I.R. Iran.*

Abstract

Background and purpose: The N-terminal Hsp90 inhibitors are promising targets for cancer treatment; however, inducing the heat shock response is one of the most significant limitations. A prominent way to overcome this limitation is by inhibiting the Hsp90 C-terminal domain.
Theoretical approach: In this study, a set of structure-based methods was engaged to predict the new C-terminal inhibitors. Since there was no human PDB structure of the Hsp90 C-terminal domain, homology modeling was done using the SWISS-MODEL server online. The 3D structure of the model was refined through energy minimization using molecular dynamics (MD) simulation for 10 ns. The active site of the created model was validated by novobiocin docking. Four steps of virtual screening, including HTVS, SP, XP, and QM/MM docking, were performed on the created library (151,332 compounds) based on 80% similarity to deguelin as the C-terminal inhibitor. The best-obtained compounds were introduced to MM-GBSA studies. Finally, the stability of the best compound was investigated using a 100 ns MD simulation.
Results/Findings: Four steps of virtual screening were performed on the created library. The extracted 46 compounds with the XP GlideScore of < -4.164 kcal/mol were introduced to MM-GBSA studies, and rescoring was done. The stability of compound CID_14018348, the best compound ($\Delta G_{binding}$ = -80.45 kcal/mol), was investigated using MD simulation.
Conclusion and implications: The compound CID_14018348 was identified as the most promising candidate through computational techniques; therefore, the computational methods outlined can be applied in the development of potent anticancer agents.

Keywords: C-terminal Hsp90 inhibitors; Deguelin; Homology modeling; MM/GBSA study; Molecular dynamic simulations; QM/MM docking; Virtual screening.

INTRODUCTION

Cancer is a major health problem characterized by the high proliferation of abnormal cells and the high expression of many proteins, such as heat shock protein 90 (Hsp90) (1). Hsp90 plays the leading role in the maturation, refolding, and renovation of misfolded proteins in more than 400 client proteins (2,3). Hsp90, as an ATP-dependent molecular chaperone, is formed of 3 main domains: the N-terminal domain is the place where ATP binding occurs (30-236), the middle domain binds to client proteins and co-chaperons (272-629), and the C-terminal domain is known as a dimerization domain (629-720) (4).

*Corresponding author: M. Abbasi
Tel: +98-7633710405, Fax: +98-7633710389
Email: mabbasi@hums.ac.ir

Access this article online	
	Website: http://rps.mui.ac.ir
	DOI: 10.4103/RPS.RPS_219_24

The maturation of client proteins is briefly performed in several steps: 1. In an open state of Hsp90 conformation, co-chaperones (Hsp70, Hsp40, and HOP) join the C-terminal domain, then transport unfolded client protein to the middle domain; 2. ATP binds to the N-terminal, and the Hsp90 conformation is closed; 3. ATP is hydrolyzed to ADP, and the client protein is matured; and 4. the mature protein is released (5-7).

Hsp90 makes about 1-2% of whole proteins in normal cells, while Hsp90 is expressed in cancer cells 2-10 times more than in normal cells (4,8). In addition, the Hsp90 conformation in the cancer phenotype is more sensitive to inhibitors (9). Based on the mentioned points and the Hsp90 effect on the maturation of several oncogenic proteins, Hsp90 inhibition could be a main strategy for cancer treatment. Hsp90 inhibitors are divided into 2 main classes: N-terminal and C-terminal inhibitors (10).

To date, more than 20 N-terminal Hsp90 inhibitors have been entered into clinical trials (11), but none of them have been effective due to various toxicities and induction of the heat shock response (HSR) (12). The HSR induction increases Hsp90 levels, heat shock factor 1, and anti-apoptotic proteins, such as Hsp70, and also starts anti-apoptotic cascades and encourages drug resistance (13,14). Therefore, studies have shifted toward inhibiting the Hsp90 C-terminal allosteric domain and protein-protein interaction inhibitors, which do not induce HSR (15).

The first compound to block the C-terminal domain of Hsp90 was novobiocin (NB), a known coumarin-based structure (4,14). Some NB derivatives, such as KU758 and KU820, were introduced with improved activity. In addition to NB derivatives, some natural compounds were known as the C-terminal Hsp90 inhibitors, such as silybin, EGCG, and deguelin, as shown in Fig. 1 (16,17).

A key point in investigating both domains (N-terminal and C-terminal) of inhibitors is that the deguelin compound is present in both. The findings showed that deguelin application in the clinic as an N-terminal inhibitor was discontinued due to its Parkinson's disease-like syndrome symptoms, despite promising anticancer activity (18,19).

Various bioinformatic techniques have been utilized to design and predict novel C-terminal inhibitors up to this point (13,16,17). In this research, a combination of computational methods was employed to identify new compounds that functioned as C-terminal Hsp90 inhibitors, utilizing the deguelin scaffold as a basis.

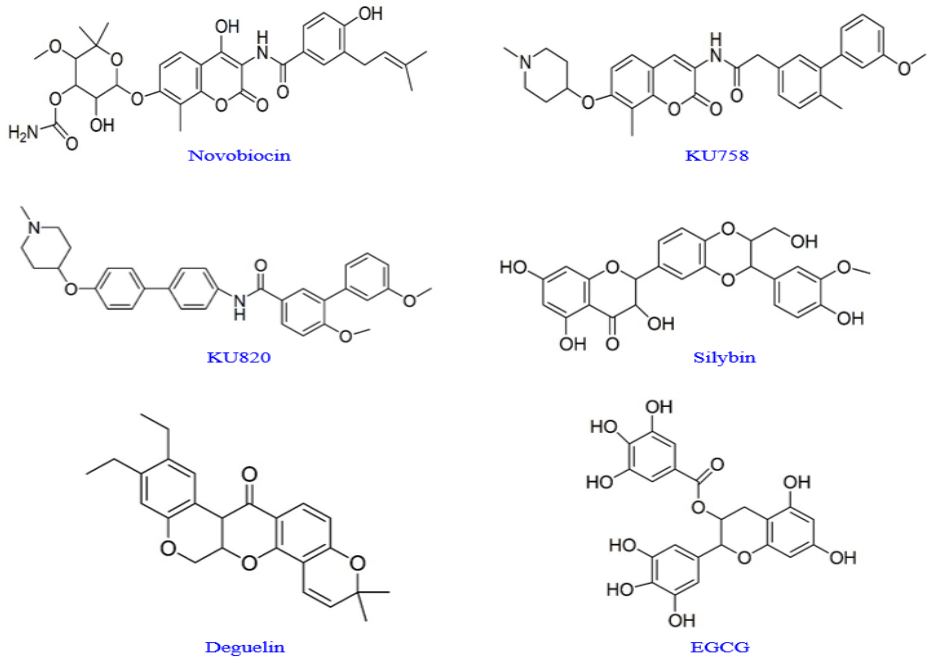

Fig. 1. Structure of several known C-terminal Hsp90 inhibitors.

METHODS

Homology modeling procedure

To date, experimental techniques like nuclear magnetic resonance (NMR) and X-ray have not determined the human crystal structure of C-terminal Hsp90 (3D structure). Homology modeling is a technique to make a 3D structure of the target protein (20). The first, a reference sequence (UniProt ID: P07900), with FASTA format, was chosen from the UniProt server (ExPASy SWISS-PROT/TrEMBL) to produce a 3D homology model of the human C-terminal Hsp90. To create a homology model, a known template sequence was required with good similarity and identity with the sequence of the human C-terminal Hsp90. The protein data bank (PDB) ID: 8FFV, with 100% identity and 61% similarity, was obtained from a template search in the SWISS-MODEL server (https://swissmodel.expasy.org/) as a template to produce the 3D structure of the human C-terminal Hsp90 (21). The alignment of the reference and template sequences was performed to understand the similar regions between the sequences, and finally, a model was built (22).

Molecular dynamics simulations and validation of the created model

In the chosen model, intense steric clashes may be created between residues due to the unusual overlapping of nonbonding atoms; thus, the molecular dynamics (MD) simulations were made by Gromacs 2021.5 (23). The protein topology parameters were made using Amber99.SB force field. The human C-terminal homology model was immersed in a dodecahedron box, and transferable intermolecular potential with 3 points (TIP3P) was chosen as a water model. To neutralize the system, the appropriate number of Cl or Na ions was replaced with solvent molecules (24). The minimization of energy was performed in a total of 100000 steps. The MD simulation was started with NVT (constant volume, temperature) and NPT (constant pressure, temperature) conditions for 1 ns. Finally, the MD run was performed for 10 ns. Then, the model validation was carried out using the PROCHECK web server (25). The favored regions of amino acid residues in agreement with stereochemistry were obtained using the Ramachandran plot. Also, the overall model quality was evaluated using the ProSA web server (26).

Library generation and virtual screening

PubChem data set is an open archive that contains almost 117 million compounds with unique chemical structures that can be used for virtual screening studies. This study utilized the PubChem online database to make a library. Deguelin compound, an Hsp90 C-terminal inhibitor, was employed as a pattern to extract compounds with 80% similarity. The extracted 151,332 compounds were saved with 3D coordinate type and structure data file (SDF) format.

Virtual screening is one of the rapid and precise methods to find novel and possible hits and leads from a data set. 151,332 compounds were introduced to the Schrodinger suite to screen in several steps (27). First, the ligand filtering was carried out in 3 stages, including 1. filtering based on the absorption, distribution, metabolism, excretion, and toxicological parameters of ligands (ADMET) using the QikProp; 2. filtering based on Lipinski's rules; 3. rejecting compounds with reactive functional groups. Then, the ligand preparation was carried out. The Epik tool made the most probable ionization states of all compounds at a pH of 7.4 ± 0.5 (28). After that, the grid box was generated, and the center of the grid box was determined to be Lys 560 as the critical amino acid in the Hsp90 C-terminal binding pocket (29). The extracted ligands were introduced to 3 steps of virtual screening as follows: 1. high-throughput virtual screening (HTVS); 2. standard precision (SP) docking; and 3. extra precision (XP) docking. In each screening process, 10% of the ligands were kept with the most negative docking score.

QM-polarized ligand docking

The QM-polarized ligand docking (QPLD) method is utilized to compute the precise charge of the ligand atoms through the application of the ab initio quantum mechanics

technique and charge of protein atoms by density functional theory, which leads to a docking study based on the hybrid quantum mechanics and molecular mechanics (QM/MM) method minimization (30). The extracted compounds from virtual screening were introduced to the Schrödinger Suite 2015 in this study. The B3LYP density functional method and 6-31G*/LACVP* basis set determined the quantum mechanics charges of ligands. Finally, XP docking was carried out, and 10 poses for each compound were reported.

Molecular mechanics/generalized Born surface area

Top QPLD docked candidates were subjected to the molecular mechanics/generalized Born surface area (MM/GBSA) approach. This method is utilized to predict the free-binding energy ($\Delta G_{binding}$) of candidate ligands within the C-terminal domain of Hsp90 with further accuracy. The MM/GBSA method merges OPLS-2005 molecular mechanics energies with a solvent-generalized Born (GB) model for polar solvation and a solvent-accessible surface area (SASA) for non-polar solvation terms (31). Consequently, the best situation of each ligand in QPLD docking was introduced to the Prime part of the Schrödinger suite 2015. The OPLS-2005 force field and variational solvent generalized born (VSGB) solvation model were utilized to calculate the MM/GBSA energy.

MD simulations

The stability of the best-obtained compound from the MM/GBSA results, deguelin and NB, as references, in the C-terminal active site of Hsp90 was computed using the MD simulation studies. The AnteChamber Python Parser Interface (ACPYPE) organized the topology parameters of the best-obtained compound and deguelin (32). The remaining steps of the MD simulation process were done in the same manner as mentioned above. Finally, the MD simulation was performed at a temperature of 300 K for 100 ns.

RESULTS

Generation of the 3D structure of the human C-terminal Hsp90

The human C-terminal Hsp 90 reference sequence with Uniport ID: P07900 and 732 amino acid residues was selected. The template (8FFV) was obtained from a template search, with 100% identity and 61% similarity. Then, the MD simulation study was performed to minimize the energy of the created structure. The secondary 3D structure of the human C-terminal Hsp90 was shown using the PyMOL tool (Fig. 2A) (33).

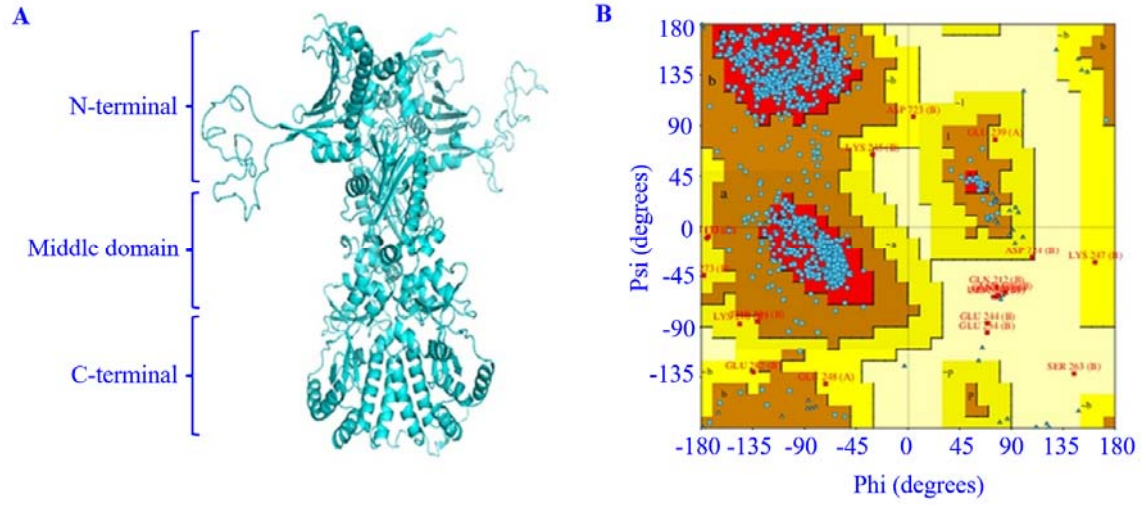

Fig. 2. (A) The secondary structure of the human homodimer of Hsp90 protein and (B) Ramachandran plot of the human homodimer of Hsp90 model.

Validation of the human homodimer of Hsp90 protein

The Ramachandran plot for the C-terminal region of the human Hsp90 model was analyzed to assess the validity of the model. This plot was generated using PROCHECK *via* the PDBsum server, and the steric clashes among amino acid residues were illustrated through a contour plot (Fig. 2B) (32). A high-quality model is expected to have more than 90% of its residues located in the most favored regions of the Ramachandran plot. The analysis revealed that 90.2% of the residues in the human Hsp90 model were situated within the core region. Consequently, the developed Hsp90 model is deemed suitable for subsequent research.

In addition, the ProSA web server was used to evaluate overall model quality (26). The Z-score plots of the created model of Hsp90 and the template protein (8FFV) are shown in Fig. 3. The z-score values of -8.64 and -9.55 were reported for the developed model of Hsp90 and the template protein, respectively. The regions with blue and light blue colors presented similar structure groups of protein obtained from NMR and X-ray methods, respectively (Fig. 3A and B). The ProSA analysis of the created model and template showed that most residues had negative sustainable energy, and very few demonstrated positive interaction energy (Fig. 3C and D).

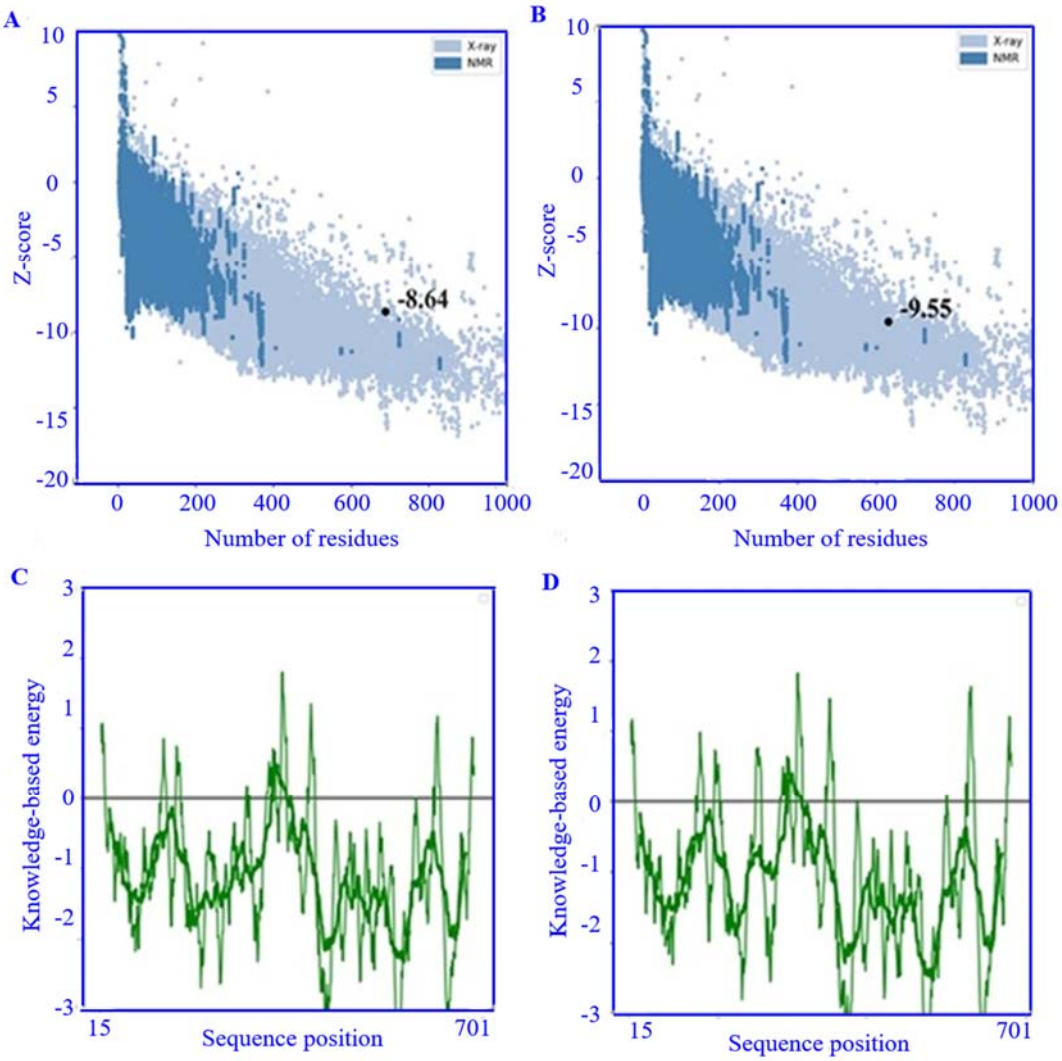

Fig. 3. (A) The Z-score of the created model; (B) the Z-score of the template protein (8FFV); (C) sequence position-based energy of the created model; (D) sequence position-based energy of the template protein (8FFV).

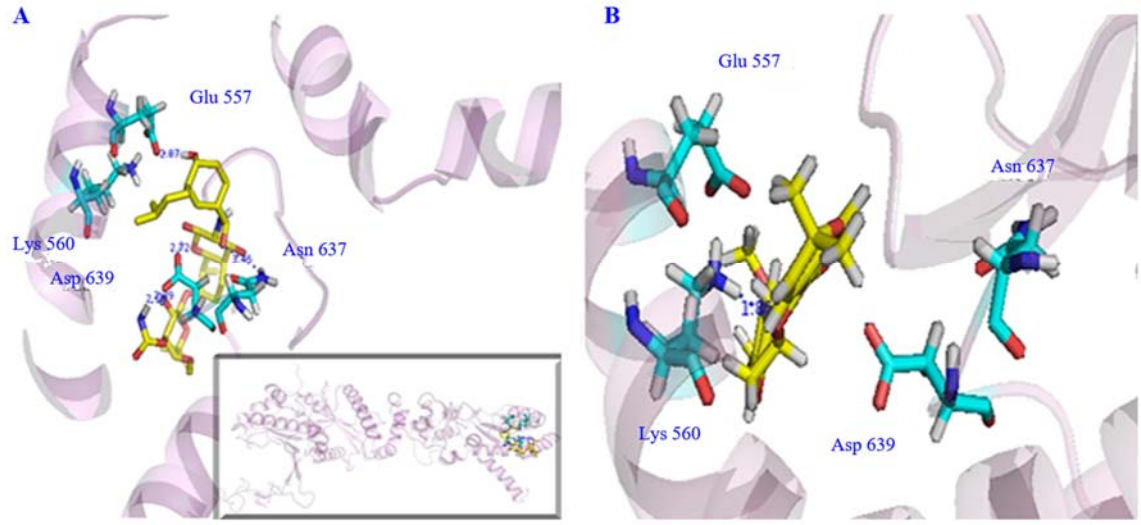

Fig. 4. (A) 3D structure of the interactions between the C-terminal domain and novobiocin; (B) 3D structure of the main interactions between the C-terminal domain and deguelin.

Docking validation

Docking validation was conducted to investigate the process of docking and predict the allosteric binding site of the C-terminal Hsp90. NB, as the known C-terminal Hsp90 inhibitor, was chosen to validate docking and investigate the primary amino acids in the C-terminal Hsp90 binding pocket. As revealed in Fig. 4A, 5 hydrogen bonds were formed between NB and active site amino acids as follows: 1. a hydrogen bond was made between the hydroxyl of noviose sugar and Asp639 (2.39 Å); 2. a hydrogen bond was seen between the amine group of the noviose carbamate and Asp639 (2.18 Å); 3. the carbonyl group of the coumarin moiety made a hydrogen bond with Asp639 (2.72 Å); 4. the carbonyl group of the amid moiety made a hydrogen bond with Asn637 (3.46 Å); and 5. a hydrogen bond was formed between the hydroxyl group of phenol ring and Glu557 (2.07 Å). Also, the main amino acids, such as Lys560, were observed at a distance less than 4 Å from NB.

Virtual screening based on molecular docking

At the beginning of screening, 3 steps of ligand filtering were performed on 151,332 compounds. The obtained compounds from the ligand filtering step were automatically introduced to the virtual screening. The structure-based virtual screening was conducted to provide more reliable results using 3 steps of the docking process (HTVS, SP, and XP). In each step of the docking process, the top 10% hit compounds with the lowest XP GlideScore were kept and introduced to the next step. Finally, 107 hit compounds were obtained from the last XP docking step based on the lowest XP GlideScore amounts. The deguelin compound was chosen as a control compound with an XP GlideScore of -3.405 kcal/mol. As shown in Fig. 4B, deguelin, as a reference, made a hydrogen bond between its oxygen atom and Lys560 at a distance of 1.85 Å, and other main amino acids were seen around it (Asp639, Asn637, and Glu557). Among all candidates, 93 compounds showed the XP GlideScore of <-3.405 kcal/mol that were introduced to further examination. Docking results for the 20 top candidates with the lowest XP GlideScore were reported in Table 1.

QPLD

QPLD calculations were done to investigate the binding mode of the resulting 93 potential hit molecules into the C-terminal Hsp90 active site. The best inhibitors were chosen in terms of their lower XP GlideScore and the more interactions with the C-terminal Hsp90 active site. Finally, 46 hit compounds with the XP GlideScore values <-4.164 kcal/mol (the value of deguelin QPLD as a reference) were identified. The QPLD results showed that these compounds sat in the deguelin and NB binding mode. QPLD results for the 20 top candidates with the lowest XP GlideScore were reported in Table 1.

Table 1. Docking and QPLD results for 20 top candidates.

Compounds	XP GScore of docking (kcal/mol)	Glide Emodel of docking (kcal/mol)	XP GScore of QPLD (kcal/mol)	Glide Emodel of QPLD (kcal/mol)
CID_40399	-7.641	-42.825	-9.137	-79.707
CID_5280647	-6.586	-41.118	-9.072	-59.208
CID_182232	-6.465	-40.904	-9.019	-57.638
CID_919792	-6.348	-42.588	-8.995	-57.600
CID_471	-6.317	-41.067	-8.896	-60.588
CID_5281642	-6.262	-39.232	-8.756	-56.085
CID_14604081	-6.148	-40.405	-8.844	-49.681
CID_5284452	-6.095	-38.835	-8.551	-47.746
CID_11095	-6.091	-40.735	-8.308	-43.080
CID_1203	-6.029	-36.297	-8.295	-45.524
CID_5281680	-5.955	-39.688	-8.276	-51.253
CID_5281692	-5.88	-40.590	-8.173	-44.287
CID_5280343	-5.794	-39.090	-7.805	-52.106
CID_5281610	-5.78	-36.370	-7.823	-55.984
CID_73160	-5.737	-39.001	-7.566	-61.628
CID_5281670	-5.729	-38.799	-7.389	-40.904
CID_68213	-5.679	-40.067	-7.186	-58.035
CID_5281701	-5.654	-37.285	-7.020	-52.297
CID_12309904	-5.621	-42.499	-6.847	-57.081
CID_5487855	-5.615	-36.526	-6.615	-54.546
Deguelin	-3.405	-20.753	-4.164	-30.979

MM/GBSA analysis

MM/GBSA calculations aim to appraise the change in enthalpy on binding; in this way, first, the simulations of all-atom are done, then the water molecules are eliminated, and the enthalpies and binding energies are computed using an implicit (Poisson-Boltzmann or Generalized Born) representation of water (31). The extracted 46 compounds from QPLD studies were rescored using the MM/GBSA method. The results showed the equilibrium of the receptor-ligand complexes. The $\Delta G_{binding}$ amounts < -27.994 kcal/mol ($\Delta G_{binding}$ of deguelin) were considered to regain the final set of hit compounds. In this screening step, 12 top-hit compounds were obtained as the C-terminal Hsp90 inhibitor. The structures of these compounds were depicted in Fig. 5. The $\Delta G_{binding}$ of the ultimately chosen hits, accompanied by the main contributions of binding energy, were presented in Table 2.

MD simulation analysis

The MD simulations for the C-terminal of Hsp90-deguelin, Hsp90-NB, and Hsp90-CID_14018348 complexes were performed for 100 ns. The stability and the fluctuations of these complexes were investigated by root-mean-square deviation (RMSD) and root-mean-square fluctuation (RMSF) plots. As shown in Fig. 6A, the RMSD of the NB complex from 1 to 100 ns remained almost constant (average 0.4241 nm), but the RMSD of Hsp90-deguelin displayed an initial increase till 25 ns. Then, it converged to a constant value, with an average value of 0.6861 nm, in the last 40 ns. The RMSD values of the CID_14018348 complex showed a fluctuation of almost 0.25 nm till 60 ns; after that, it remained nearly constant with an average value of 0.6384 nm.

The RMSF of the protein backbone of all systems was analyzed and represented in Fig. 6B. All 3 systems (Hsp90-deguelin, Hsp90-NB, and Hsp90-CID_14018348 complexes) exhibited a similar fluctuation pattern across all 243 amino acids, except amino acids 650 to 675 in the Hsp90-NB complex. The main amino acids 510 to 595 and 635 to 650 showed the lowest fluctuation.

The compactness of all systems was determined using radius of gyration (Rg) (Fig. 6C). The obtained average Rg value for the Hsp90-NB complex was 1.9763 nm. The highest fluctuation was observed in the Hsp90-deguelin complex in the first 10 ns. After 40 ns, the Rg pattern of Hsp90-deguelin and Hsp90-CID_14018348 complexes was aligned together. Figure 6D illustrates the number of hydrogen bonds established among the Hsp90-deguelin, Hsp90-NB, and Hsp90-CID_14018348 complexes throughout a 100 ns MD simulation. The fluctuations in the number of hydrogen bonds for these complexes were recorded between 0 and 6.

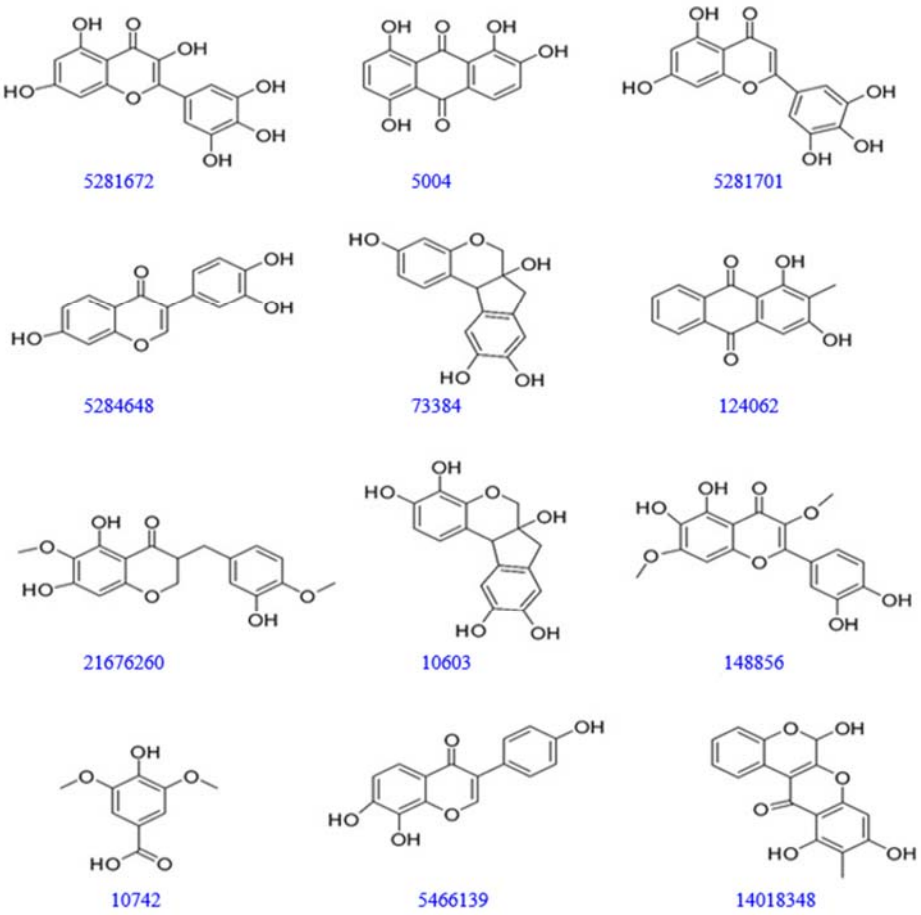

Fig. 5. Chemical structures of the selected ligands from MM/GBSA calculations as the C-terminal of Hsp90 inhibitors.

Table 2. Results of the binding free energy of the extracted ligands by MM/GBSA studies in the C-terminal pocket of Hsp90 protein.

Compounds	$\Delta G_{binding}$	$\Delta G_{Coulomb}$	ΔG_{Lipo}	ΔG_{SolvGB}	ΔG_{vdW}
CID_5281672	-32.83	-32.91	-5.92	25.42	-17.78
CID_5004	-52.56	-18.94	-15.46	16.29	-33.47
CID_5281701	-30.52	-15.84	-15.11	14.99	-29.65
CID_5284648	-55.04	-15.62	-10.72	11.45	-21.29
CID_73384	-32.22	-6.82	-12.70	13.76	-25.32
CID_124062	-28.61	-18.56	-11.76	9.28	-24.83
CID_21676260	-34.67	-20.84	-12.94	26.32	-26.58
CID_10742	-28.79	14.84	-19.25	-33.04	-33.34
CID_148856	-31.84	-16.66	-6.36	15.68	-21.84
CID_10603	-29.60	-16.7	-7.73	15.81	-19.84
CID_5466139	-29.48	-8.36	-11.45	11.22	-19.00
CID_14018348	-80.45	-21.93	-29.62	15.49	-46.90
Deguelin	-27.99	-4.45	-17.82	23.59	-37.15

ΔG, Binding free energy.

The Gibbs free energy landscape (FEL) was determined through the projections of the first (PC1) and second (PC2) eigenvectors. Figure 7 represents the two-dimensional FEL plot for the C-terminal backbone of Hsp90 in association with the CID_14018348 compound. In the corresponding free energy contour map, red colour indicated lower energy levels, whereas dark blue colour denoted higher energy levels.

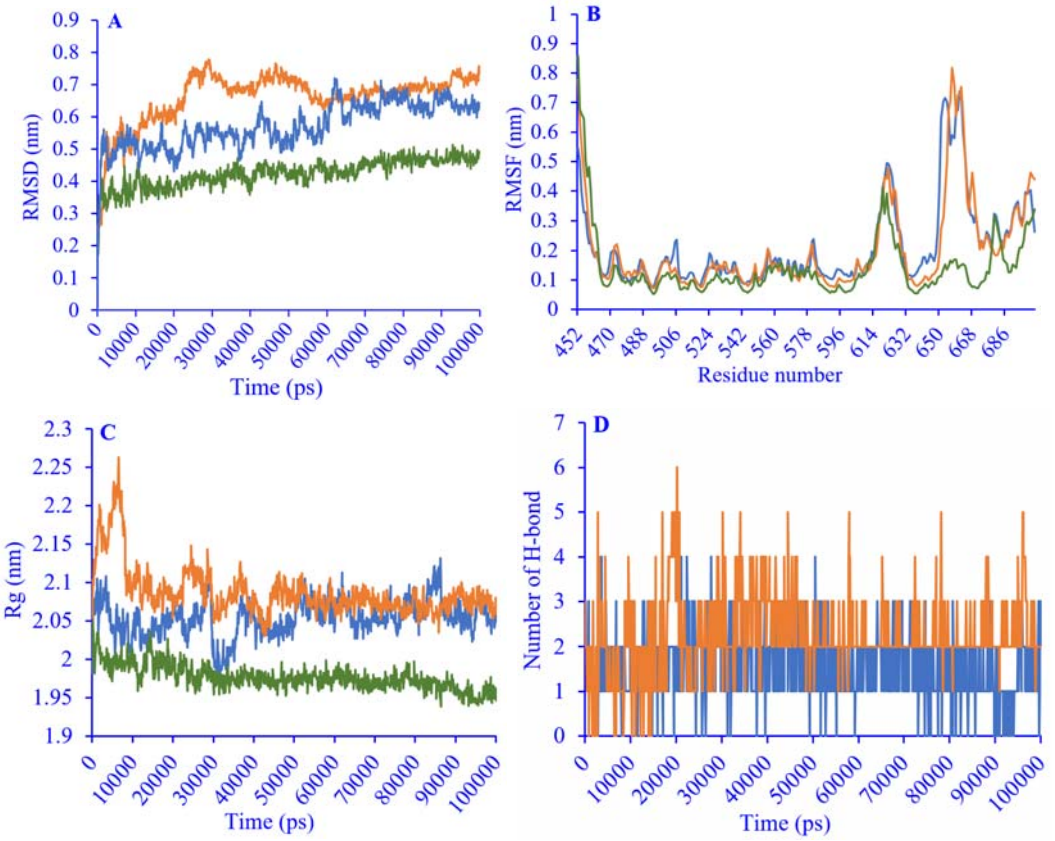

Fig. 6. (A) The RMSD profile of the C-terminal of Hsp90 backbone in complex with deguelin, NB, and CID_14018348 as a function of simulation time; (B) the RMSF plot of the C-terminal of Hsp90 backbone in complex with deguelin, NB, CID_14018348; (C) Rg plot of the C-terminal of Hsp90 backbone in complex with deguelin, NB, CID_14018348; (D) number of hydrogen bonds established in the Hsp90-deguelin and Hsp90-CID_14018348 complexes during 100 ns simulation. Deguelin, NB, and CID_14018348 were specified by orange, green, and blue, respectively. RMSD, Root-mean-square deviation; RMSF, root-mean-square fluctuation; Rg, radius of gyration; NB, novobiocin.

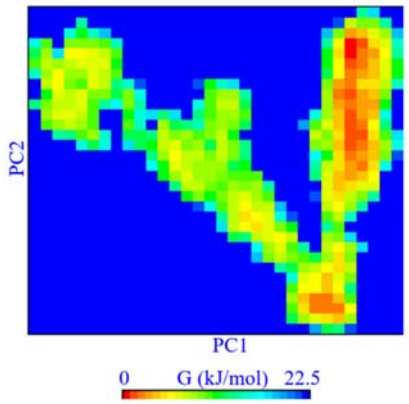

Fig. 7. The Gibbs free energy landscape plot for the C-terminal backbone of Hsp90 in complex with the CID_14018348 compound during 100 ns molecular dynamics simulations. PC_1, The first principal component; PC_2, the second principal component.

DISCUSSION

In this study, various bioinformatic techniques were employed to predict new C-terminal Hsp90 inhibitors based on the deguelin scaffold. First, the three-dimensional structure of human C-terminal Hsp90 was generated using homology modeling. The resulting model was evaluated using Ramachandran plots and Z-scores. The evaluation indicated that the model fell within the acceptable ranges established by X-ray and NMR studies. Next, a series of structure-based virtual screenings, including HTVS, SP, XP, and QPLD, were conducted on a library containing 151,332 compounds. From this analysis, 46 compounds with the lowest GlideScores (< -4.164 kcal/mol) and the greatest interaction between the ligand and the protein were selected for further investigation using MM/GBSA calculations. Ultimately, 12 top-hit compounds were identified based on their $\Delta G_{binding}$ to deguelin (< -27.994 kcal/mol).

Among the 12 hit compounds, the lowest $\Delta G_{binding}$ was observed in compound CID_14018348, which had a $\Delta G_{binding}$ value of -80.45 kcal/mol. In this compound, the most significant contributions to binding energy came from the van der Waals interactions (-46.90 kcal/mol) and the lipophilic interactions (-29.62 kcal/mol). This compound formed 4 hydrogen bonds with 3 amino acids, including Lys560 (distances of 2.57 and 2.61 Å), Gln561 (distance of 2.27 Å), and Leu592 (distance of 1.89 Å). Additionally, a π-cation interaction was observed between the aromatic ring and Lys513.

As shown in Table 2, the MM/GBSA results indicated that compound CID_5284648 bound to the C-terminal binding site of Hsp90 with a $\Delta G_{binding}$ value of -55.04 kcal/mol. The primary contributors to the $\Delta G_{binding}$ in this compound were the van der Waals interactions (-21.29 kcal/mol), coulombic interactions (-15.62 kcal/mol), and lipophilic interactions (-10.72 kcal/mol). Three hydroxyl groups from the phenol rings were crucial for forming hydrogen bonds with Asp639 and Pro552, at distances of 1.88, 1.76, and 2.18 Å. A π-cation interaction was also observed between the aromatic ring and His514.

The ligand CID_5004 bound in the C-terminal region of the Hsp90 binding pocket, displaying a $\Delta G_{binding}$ value of -52.56 kcal/mol (Table 2). The main contributors to the energy in compound CID_5004 were the van der Waals interactions (-33.47 kcal/mol), coulombic interactions (-18.94 kcal/mol), and lipophilic interactions (-15.46 kcal/mol). This compound formed 6 hydrogen bonds with amino acids Asp656, Ser658, Lys564, Lys560, Glu557, and Lys513. Additionally, a π-cation interaction occurred between the aromatic ring and Arg510.

The MD simulation results (RMSD, RMSF, and Rg) were compared with the results of deguelin and NB as references. The analysis of the results showed that compound CID_14018348 remained stable in the active site, similar to deguelin and NB. The RMSF plot indicated that the primary amino acids ranging from positions 510 to 639 in the protein across the 3 complexes exhibited greater stability. Notably, Asp656 and Ser658 demonstrated enhanced stability in the presence of NB when compared to deguelin and compound CID_14018348.

CONCLUSION

Herein, the current study performed a structure-based virtual screening to find new compounds with the potential for inhibiting the C-terminal domain of Hsp90. After 5 steps of virtual screening on 151,332 compounds, 3 compounds were introduced as the C-terminal domain of Hsp90 inhibitors. Using the final screening, 3 compounds, CID_14018348, CID_5284648, and CID_5004, showed the most negative value of $\Delta G_{binding}$ within the binding pocket of the C-terminal of Hsp90 protein. The investigation of MM/GBSA calculations showed that the van der Waals force played the main role in the $\Delta G_{binding}$ between the ligand and the C-terminal domain of Hsp90, using the hydroxyl groups in the structure. The best compound with the $\Delta G_{binding}$ value of -80.45 kcal/mol (CID_14018348) was chosen and subjected to the MD simulation study to identify the binding resistance and stability. MD studies confirmed the stability of all predicted compounds in the C-terminal active site. Therefore, the present study may be the basis for further studies on the C-terminal domain of Hsp90 as a goal for cancer inhibition.

Acknowledgements

This work was financially supported by Hormozgan University of Medical Sciences (Grant No. 4000033).

Conflict of interest statement

The authors declared no conflict of interest in this study.

Authors' contributions

M. Abbasi participated in the design of the study, drafted the manuscript, and also provided financial and administrative support; S. Talaei performed molecular docking and molecular dynamics simulation; G. Farshidfar provided financial and administrative support. All authors read and approved the final version of the manuscript.

REFERENCES

1. Liu J, Shu H, Xia Q, You Q, Wang L. Recent developments of HSP90 inhibitors: an updated patent review (2020-present). Expert Opin Ther Pat. 2024;34(1-2):1-15. DOI: 10.1080/13543776.2024.2327295.
2. Hoter A, El-Sabban ME, Naim HY. The HSP90 family: structure, regulation, function, and implications in health and disease. Int J Mol Sci. 2018;19(9):2560,1-33. DOI: 10.3390/ijms19092560.
3. Campanella C, Pace A, Caruso Bavisotto C, Marzullo P, Marino Gammazza A, Buscemi S, *et al*. Heat shock proteins in Alzheimer's disease: role and targeting. Int J Mol Sci. 2018;19(9):2603,1-22. DOI: 10.3390/ijms19092603.
4. Shadrack DM, Swai HS, Hassanali A. A computational study on the role of water and conformational fluctuations in Hsp90 in response to inhibitors. J Mol Graph Model. 2020;96:107510. DOI: 10.1016/j.jmgm.2019.107510.
5. Mielczarek-Lewandowska A, Hartman ML, Czyz M. Inhibitors of HSP90 in melanoma. Apoptosis. 2020; 25(1-2):12-28. DOI: 10.1007/s10495-019-01577-1.
6. Toss A, Venturelli M, Peterle C, Piacentini F, Cascinu S, Cortesi L. Molecular biomarkers for prediction of targeted therapy response in metastatic breast cancer: trick or treat? Int J Mol Sci. 2017;18(1):85,1-24. DOI: 10.3390/ijms18010085.
7. Alimardan Z, Abbasi M, Khodarahmi G, Kashfi K, Hasanzadeh F, Aghaei M. Identification of new small molecules as dual FoxM1 and Hsp70 inhibitors using computational methods. Res Pharm Sci. 2022;17(6):635-656. DOI: 10.4103/1735-5362.359431.
8. Alosaimy AM, Abouzied AS, Alsaedi AMR, Alafnan A, Alamri A, Alamri MA, *et al*. Discovery of novel indene-based hybrids as breast cancer inhibitors targeting Hsp90: synthesis, bio-evaluation and molecular docking study. Arab J Chem. 2023;16(4):104569,1-13. DOI: 10.1016/j.arabjc.2023.104569.
9. Kamal A, Thao L, Sensintaffar J, Zhang L, Boehm MF, Fritz LC, *et al*. A high-affinity conformation of Hsp90 confers tumour selectivity on Hsp90 inhibitors. Nature. 2003;425(6956):407-410. DOI: 10.1038/nature01913.
10. Miller DJ, Fort PE. Heat shock proteins regulatory role in neurodevelopment. Front Neurosci. 2018;12:821,1-15. DOI: 10.3389/fnins.2018.00821.
11. Sanchez J, Carter TR, Cohen MS, Blagg BSJ. Old and new approaches to target the Hsp90 chaperone. Curr Cancer Drug Targets. 2020;20(4):253-270. DOI: 10.2174/1568009619666191202101330.
12. Jaeger AM, Whitesell L. HSP90: enabler of cancer adaptation. Annu Rev Cancer Biol. 2019;3:275-297. DOI: 10.1146/annurev-cancerbio-030518-055533.
13. Tomašič T, Durcik M, Keegan BM, Skledar DG, Zajec Ž, Blagg BSJ, *et al*. Discovery of novel Hsp90 C-terminal inhibitors using 3D-pharmacophores derived from molecular dynamics simulations. Int J Mol Sci. 2020;21(18):6898,1-22. DOI: 10.3390/ijms21186898.
14. Bhatia S, Diedrich D, Frieg B, Ahlert H, Stein S, Bopp B, *et al*. Targeting HSP90 dimerization *via* the C terminus is effective in imatinib-resistant CML and lacks the heat shock response. Blood. 2018;132(3):307-320. DOI: 10.1182/blood-2017-10-810986.
15. Dernovšek J, Zajec Ž, Durcik M, Mašič LP, Gobec M, Zidar N, *et al*. Structure-activity relationships of benzothiazole-based Hsp90 C-terminal-domain inhibitors. Pharmaceutics. 2021;13(8):1283,1-30. DOI: 10.3390/pharmaceutics13081283.
16. Zajec Ž, Dernovšek J, Gobec M, Tomašič T. In silico discovery and optimisation of a novel structural class of Hsp90 C-terminal domain inhibitors. Biomolecules. 2022;12(7):884,1-23. DOI: 10.3390/biom12070884.
17. Donnelly A, Blagg BSJ. Novobiocin and additional inhibitors of the Hsp90 C-terminal nucleotide-binding pocket. Curr Med Chem. 2008;15(26):2702-2717. DOI: 10.2174/092986708786242895.
18. Chang DJ, An H, Kim KS, Kim HH, Jung J, Lee JM, *et al*. Design, synthesis, and biological evaluation of novel deguelin-based heat shock protein 90 (HSP90) inhibitors targeting proliferation and angiogenesis. J Med Chem. 2012;55(24):10863-10884. DOI: 10.1021/jm301488q.
19. Lin ZY, Yun QZ, Wu L, Zhang TW, Yao TZ. Pharmacological basis and new insights of deguelin concerning its anticancer effects. Pharmacol Res. 2021;174:105935. DOI: 10.1016/j.phrs.2021.105935.

20. Lanka G, Bathula R, Bhargavi M, Potlapally SR. Homology modeling and molecular docking studies for the identification of novel potential therapeutics against human PHD3 as a drug target for type 2 diabetes mellitus. J Drug Delivery Ther. 2019;9(4):265-273. DOI: 10.22270/jddt.v9i4.3039.
21. Cuyàs E, Verdura S, Micol V, Joven J, Bosch-Barrera J, Encinar JA, *et al*. Revisiting silibinin as a novobiocin-like Hsp90 C-terminal inhibitor: computational modeling and experimental validation. Food Chem Toxicol. 2019;132:110645,1-12. DOI: 10.1016/j.fct.2019.110645.
22. Schrodinger L. Prime. Version 3.9. New York (NY); 2015.
23. Abraham MJ, Murtola T, Schulz R, Páll S, Smith JC, Hess B, *et al*. GROMACS: high performance molecular simulations through multi-level parallelism from laptops to supercomputers. SoftwareX. 2015;1-2:19-25. DOI: 10.1016/j.softx.2015.06.001.
24. Jorgensen WL, Chandrasekhar J, Madura JD, Impey RW, Klein ML. Comparison of simple potential functions for simulating liquid water. J Chem Phys.1983;79(2):926-935. DOI: 10.1063/1.445869.
25. Laskowski RA, MacArthur MW, Moss DS, Thornton JM. PROCHECK: a program to check the stereochemical quality of protein structures. J Appl Cryst. 1993;26(2):283-291. DOI: 10.1107/S0021889892009944.
26. Wiederstein M, Sippl MJ. ProSA-web: interactive web service for the recognition of errors in three-dimensional structures of proteins. Nucleic Acids Res. 2007;35(suppl_2): W407-W410. DOI: 10.1093/nar/gkm290.
27. Schrödinger L. Schrödinger Release 2015-3: LigPrep. Schrödinger LLC, New York, NY; 2015.
28. Epik. Version 3.4. Schrödinger LLC. New York, NY; 2015.
29. Matts RL, Dixit A, Peterson LB, Sun L, Voruganti S, Kalyanaraman P, *et al*. Elucidation of the Hsp90 C-terminal inhibitor binding site. ACS Chem Biol. 2011;6(8):800-807. DOI: 10.1021/cb200052x.
30. Abbasi M, Mahboubi-Rabbani M, Kashfi K, Sadeghi-Aliabadi H. Prediction of dual NF-κB/IκB inhibitors using an integrative in-silico approaches. J Biomol Struct Dyn. 2023;41(23):14164-14178. DOI: 10.1080/07391102.2023.2178507.
31. Mobley DL, Dill KA. Binding of small-molecule ligands to proteins:"what you see" is not always "what you get". Structure. 2009;17(4):489-498. DOI: 10.1016/j.str.2009.02.010.
32. Sousa da Silva AW, Vranken WF. ACPYPE-AnteChamber PYthon Parser interface. BMC Res Notes. 2012;5:367,1-8. DOI: 10.1186/1756-0500-5-367.
33. Makarewicz T, Kaźmierkiewicz R. Molecular dynamics simulation by GROMACS using GUI plugin for PyMOL. J Chem Inf Model. 2013;53(5):1229-1234. DOI: 10.1021/ci400071x.